

# Details of Potential Energy Surfaces Involving C–C Bond Activation: Reactions of Fe<sup>+</sup>, Co<sup>+</sup>, and Ni<sup>+</sup> with Acetone

Catherine J. Carpenter, Petra A. M. van Koppen,\* and Michael T. Bowers\*

Contribution from the Department of Chemistry, University of California, Santa Barbara, California 93106

Received March 28, 1995<sup>⊗</sup>

**Abstract:** Product kinetic energy release distributions (KERDs) for reactions of Fe<sup>+</sup>, Co<sup>+</sup>, and Ni<sup>+</sup> with acetone to eliminate C<sub>2</sub>H<sub>6</sub> and CO have been measured. These distributions are statistical and are very sensitive to the energy of the rate-limiting transition state. We argue this transition state is most likely due to initial C–C bond insertion. The rate-limiting transition state acts to restrict high angular momentum reactant collision complexes from going on to products, thereby reducing the average kinetic energy released. By modeling the experimental KERDs, the rate-limiting transition state was determined to lie in the range of 9 ± 3 kcal/mol below the energy of the M<sup>+</sup> + acetone reactants for all three metal ions. Bond energies for M<sup>+</sup>–CO and M<sup>+</sup>–C<sub>2</sub>H<sub>6</sub> have also been determined: D<sub>0</sub>(Co<sup>+</sup>–CO) = 39.1 ± 3 kcal/mol, D<sub>0</sub>(Fe<sup>+</sup>–C<sub>2</sub>H<sub>6</sub>) = 17.9 ± 3 kcal/mol, and D<sub>0</sub>(Ni<sup>+</sup>–C<sub>2</sub>H<sub>6</sub>) = 28.7 ± 3 kcal/mol. In addition, modeling the experimental KERDs indicates that the MC<sub>2</sub>H<sub>6</sub><sup>+</sup> product formed in the reaction of M<sup>+</sup> with acetone is nearly exclusively an ethane adduct, with a maximum 10–15% of the dimethyl complex being formed. Finally, arguments relating the initial rate-limiting transition state to the C–H bond activation transition state in propane are made and suggest that the C–C bond activation transition state in small alkanes is 6 ± 5 kcal/mol higher in energy than C–H bond activation.

## Introduction

One of the primary goals in organometallic chemistry is to determine the factors that promote  $\sigma$ -bond activation at transition metal centers. Of particular interest is the activation of C–H and C–C bonds in small hydrocarbons both because of the enormous practical importance to the petroleum industry and because of the fundamental importance of  $\sigma$  bonds as among the simplest, strongest, and most ubiquitous of chemical bonds. A growing and important aspect of these studies is the use of bare transition metal ions as probes of the  $\sigma$ -bond activation process and in recent years a significant number of papers have been published in this general area.<sup>1–14</sup> One of the intriguing aspects of this work is that at thermal energy all of the chemistry induced by transition metals in propane results from initial C–H rather than initial C–C bond activation.<sup>15</sup> At first glance this

is a curious result because C–C bonds in alkanes are weaker than C–H bonds<sup>16</sup> suggesting they should at least compete as sites of reaction initiation.

An important clue to  $\sigma$ -bond activation in alkanes comes from the fact that larger alkanes react faster than smaller ones despite the fact that C–H (and C–C) bond strengths are essentially independent of alkane size. For example, at thermal energies, Co<sup>+</sup> does not react with methane and ethane,<sup>17,18</sup> and it reacts only slowly with propane<sup>14,15,17</sup> and much faster with larger alkanes.<sup>19</sup> The fact that CH<sub>4</sub> is unreactive is reasonable since all reaction channels are endoergic, but H<sub>2</sub> elimination from C<sub>2</sub>H<sub>6</sub> by Co<sup>+</sup> is exoergic by 11 kcal/mol<sup>20</sup> yet is not observed. The slow reactivity of Co<sup>+</sup> (and several other first row metal ions) with C<sub>3</sub>H<sub>8</sub> to eliminate both H<sub>2</sub> and CH<sub>4</sub> provided a unique opportunity to probe the kinetically (and dynamically) important parts of the potential energy surface in that system.<sup>15</sup> These studies allowed unambiguous determination that at thermal energy initial C–H bond activation transition states (TS's) are responsible for all the chemistry observed and that C–C bonds are activated only after M<sup>+</sup> has inserted initially into a C–H bond. This initial C–H insertion transition state also turns out to be rate determining despite the fact other important transition states must occur along the reaction coordinate.

\* Author to whom correspondence should be addressed.

<sup>⊗</sup> Abstract published in *Advance ACS Abstracts*, October 15, 1995.

(1) For a review, see: Eller, K.; Schwarz, H. *Chem. Rev.* **1991**, *91*, 1121 and references therein.

(2) Weisshaar, J. C. *Acc. Chem. Res.* **1993**, *26*, 213.

(3) Weisshaar, J. C. In *Advances in Chemical Physics*; Ng, C., Ed.; Wiley-Interscience: New York, 1992; Vol. 82, pp 213–261.

(4) Hanton, S. D.; Noll, R. J.; Weisshaar, J. C. *J. Chem. Phys.* **1992**, *96*, 5176.

(5) Sanders, L.; Hanton, S. D.; Weisshaar, J. C. *J. Chem. Phys.* **1990**, *92*, 3498.

(6) Armentrout, P. B. *Science* **1991**, *251*, 175.

(7) Armentrout, P. B. *Annu. Rev. Phys. Chem.* **1990**, *41*, 313.

(8) Georgiadis, R.; Fisher, E. R.; Armentrout, P. B. *J. Am. Chem. Soc.* **1989**, *111*, 4251.

(9) Schultz, R. H.; Elkind, J. L.; Armentrout, P. B. *J. Am. Chem. Soc.* **1988**, *110*, 411.

(10) Aristov, N.; Armentrout, P. B. *J. Phys. Chem.* **1987**, *91*, 6178.

(11) Houriet, R.; Halle, L. F.; Beauchamp, J. L. *Organometallics* **1983**, *2*, 1818.

(12) van Koppen, P. A. M.; Kemper, P. R.; Bowers, M. T. *J. Am. Chem. Soc.* **1992**, *114*, 1083.

(13) van Koppen, P. A. M.; Kemper, P. R.; Bowers, M. T. *J. Am. Chem. Soc.* **1992**, *114*, 10941.

(14) van Koppen, P. A. M.; Kemper, P. R.; Bowers, M. T. In *Organometallic Ion Chemistry*; Freiser, B. S., Ed.; Kluwer Academic Publishers: The Netherlands, in press.

(15) (a) van Koppen, P. A. M.; Brodbelt-Lustig, J.; Bowers, M. T.; Dearden, D. V.; Beauchamp, J. L.; Fisher, E. R.; Armentrout, P. B. *J. Am. Chem. Soc.* **1991**, *113*, 2359. (b) van Koppen, P. A. M.; Brodbelt-Lustig, J.; Bowers, M. T.; Dearden, D. V.; Beauchamp, J. L.; Fisher, E. R.; Armentrout, P. B. *J. Am. Chem. Soc.* **1990**, *112*, 5663. (c) van Koppen, P. A. M.; Bowers, M. T.; Fisher, E. R.; Armentrout, P. B. *J. Am. Chem. Soc.* **1994**, *116*, 3780.

(16) Lias, S. G.; Bartmess, J. E.; Liebman, J. F.; Holmes, J. L.; Levin, R. D.; Mallard, W. G. *J. Phys. Chem. Ref. Data* **1988**, *17* (Suppl. 1).

(17) Tonkyn, R.; Ronan, M.; Weisshaar, J. C. *J. Phys. Chem.* **1988**, *92*, 92.

(18) Armentrout, P. B.; Beauchamp, J. L. *J. Am. Chem. Soc.* **1981**, *103*, 784.

(19) Jacobson, D. B.; Freiser, B. S. *J. Am. Chem. Soc.* **1983**, *105*, 5197.

(20) Measurement of D<sub>0</sub>(Co<sup>+</sup>–C<sub>2</sub>H<sub>4</sub>) indicates that H<sub>2</sub> loss from Co<sup>+</sup> + ethane is exothermic (see refs 14 and 21).

(21) Hanratty, M. A.; Beauchamp, J. L.; Illies, A. J.; van Koppen, P.; Bowers, M. T. *J. Am. Chem. Soc.* **1988**, *110*, 1.

The simplest way to picture what is happening in these systems is to reduce complex features of the complete potential energy surface (PES) to those essential features that can be readily probed by experiment and modeled by theory. This "reaction coordinate" approach yields the following picture. As  $M^+$  approaches the alkane, the long-range ion-induced dipole forces generate an attraction between the ion and neutral. Consequently, the first feature encountered along the reaction coordinate is a potential well associated with the  $M^+$ -alkane adduct. If the system is to proceed along the reaction coordinate, the metal ion must approach the alkane and attempt to insert into a C-H (or C-C) bond. Initially, the energy rises rapidly due to electrostatic repulsion. However, as the metal ion approaches closer, new "chemical" forces associated with covalent bond breaking and forming become involved. The balancing of these various forces eventually yields an energy saddle point along the reaction coordinate at the C-H (or C-C) insertion transition state. If the energy associated with this TS is above the asymptotic  $M^+$ /alkane reactant energy, then at thermal energy the system is simply reflected and returns to reactants. If the TS energy is below the reactant energy then the reaction might occur. Consequently, we can conclude that in alkanes the C-H insertion TS is above the  $M^+$ / $C_2H_6$  asymptotic energy but below the  $M^+$ / $C_3H_8$  energy.

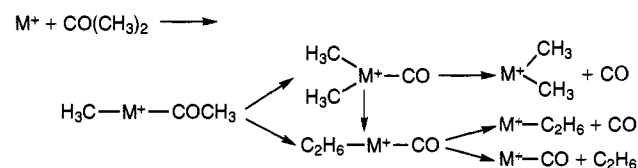
Since the nature of the bonding in the transition state is essentially identical for  $C_2H_6$  and  $C_3H_8$ , the lowering of the  $M^+$ / $C_3H_8$  TS relative to the  $M^+$ / $C_2H_6$  TS must be due to a deeper  $M^+$ - $C_3H_8$  adduct well. Experiments indicate that this is the case for first row metals<sup>15,22</sup> as does theory.<sup>23</sup> It also makes sense simply because the polarizability increases with alkane size and since the primary interaction between  $M^+$  and the alkane adduct is electrostatic, the adduct well depth should correlate with alkane polarizability.

It is not completely clear why C-C bond activation is not observed in small alkanes. The only experimental evidence suggests C-C bond activation in  $Fe^+$ / $C_3H_8$  is  $\sim 8$  kcal/mol higher in energy than C-H bond activation.<sup>24</sup> Theory<sup>25,26</sup> suggests that metals have more difficulty activating C-C bonds in alkanes because the  $sp^3$ -hybrid orbitals on carbon are highly directional and resist the reorientation required in the transition state (relative to the spherical s orbital on hydrogen). Regardless of the reason, so far we have been unable to clearly characterize C-C bond activation using alkanes, hence another system needs to be found.

A promising candidate is acetone. Prior studies<sup>27,28</sup> have shown that  $Fe^+$ ,  $Co^+$ , and  $Ni^+$  readily react with acetone to exoergically eliminate CO and  $C_2H_6$ . Further, all reaction channels that arise from C-H bond activation are endoergic. A possible reaction mechanism to explain the observed products is given in Scheme 1. An important aspect of Scheme 1 is the assumption that C-C bond insertion initiates the metal induced chemistry, implying that the C-C bond activation TS in  $M^+$ /acetone must be below the asymptotic  $M^+$ /acetone energy.

There are two possible reasons this TS may be much lower in energy for acetone than for propane. First, acetone is a polar

### Scheme 1



molecule. Consequently, ion-dipole forces will result in a substantially deeper initial "electrostatic complex" well for acetone than for propane. Theory<sup>23,29</sup> suggests the added stabilization may be as great as 20 kcal/mol.

The second reason is that the C-C bond in acetone is 6 kcal/mol weaker than the C-C bond in propane.<sup>16</sup> This relative bond weakening may be due to either the reduced overlap of the  $sp^3$ -hybridized methyl carbon with the  $sp^2$ -hybridized carbonyl carbon and/or the electron-withdrawing nature of the carbonyl group. The carbonyl group may actually assist in initial C-C bond activation by this inductive effect, further lowering the activation energy barrier associated with C-C bond activation.

Our approach in this study is to measure accurate kinetic energy release distributions<sup>15,30,31</sup> (KERDs) and to model them with statistical phase space theory.<sup>32</sup> We will consider initial C-C bond activation and several other processes as sources of the rate-limiting TS. We will also address the question of whether  $M(CH_3)_2^+$  or  $M^+ \cdot C_2H_6$  products dominate the CO elimination channel and question whether or not the  $OC-M^+-(CH_3)_2$  intermediate actually plays a role in the chemistry observed at thermal energies. Analysis of the KERD data will allow accurate determination of the energy of the rate-limiting TS for  $M = Fe, Co,$  and  $Ni$ . Further, by using the literature value of the  $Co^+-C_2H_6$  bond energy<sup>22</sup> and relative  $M^+-CO$  bond energies calculated by theory,<sup>33</sup> we will determine a self-consistent set of bond energies for  $Fe^+, Co^+,$  and  $Ni^+$  bound to CO and  $C_2H_6$ .

### Experimental Section

The KERDs were obtained using a reverse geometry double focusing mass spectrometer (VG Instruments ZAB-2F)<sup>34</sup> with a home-built temperature- and pressure-variable source. Metal ions were formed by electron impact on  $Fe(CO)_5, Co(CO)_3NO,$  and  $Ni(CO)_4$ . Source temperatures were maintained near 273 K to minimize decomposition of metal-containing compounds on insulating surfaces. The  $M^+$ -acetone adducts were formed by collision between the metal ions and acetone in the source. Source pressures were kept at approximately  $10^{-3}$  Torr to avoid collisional stabilization of the adduct. The ions were accelerated to 8 keV after leaving the source and mass selected by the magnetic sector. The metastable ions decomposed in the second field-free region between the magnetic and electric sectors and the ionic fragments were energy analyzed by scanning the electric sector. The metastable peaks were collected using a multichannel analyzer and were differentiated to obtain the center of mass product kinetic release energy

(29) Perry, J. K. Personal communication.

(30) van Koppen, P. A. M.; Jacobson, D. B.; Illies, A. J.; Bowers, M. T.; Hanratty, M. A.; Beauchamp, J. L. *J. Am. Chem. Soc.* **1989**, *111*, 1991.

(31) (a) van Koppen, P. A. M.; Bowers, M. T.; Beauchamp, J. L. *Organometallics* **1990**, *9*, 625. (b) van Koppen, P. A. M.; Bowers, M. T.; Beauchamp, J. L.; Dearden, D. V. In *Bonding Energetics in Organometallic Compounds*; Marks, T. J., Ed.; ACS Symposium Series 428; American Chemical Society: Washington, DC, 1990; pp 34-54.

(32) (a) Pechukas, P.; Light, J. C.; Rankin, C. J. *Chem. Phys.* **1966**, *44*, 794. (b) Nikitin, E. *Theor. Exp. Chem. (Eng. Transl.)* **1965**, *1*, 285. (c) Chesnavich, W. J.; Bowers, M. T. *J. Am. Chem. Soc.* **1976**, *98*, 8301. (d) Chesnavich, W. J.; Bowers, M. T. *J. Chem. Phys.* **1978**, *68*, 901. (e) Chesnavich, W. J.; Bowers, M. T. *Prog. React. Kinet.* **1982**, *11*, 137.

(33) Barnes, L. A.; Rosi, M.; Bauschlicher, C. W., Jr. *J. Chem. Phys.* **1990**, *93*, 609.

(34) Morgan, R. P.; Benyon, J. H.; Bateman, R. H.; Green, B. N. *Int. J. Mass Spectrom. Ion Phys.* **1978**, *28*, 171.

(22) Kemper, P. R.; Bushnell, J.; van Koppen, P.; Bowers, M. T. *J. Phys. Chem.* **1993**, *97*, 1810.

(23) Perry, J. K.; Ohanessian, G.; Goddard, W. A., III *J. Phys. Chem.* **1993**, *97*, 5238.

(24) Schultz, R. H.; Armentrout, P. B. *J. Am. Chem. Soc.* **1991**, *113*, 729.

(25) (a) Low, J. J.; Goddard, W. A., III *J. Am. Chem. Soc.* **1984**, *106*, 8321. (b) Low, J. J.; Goddard, W. A., III *Organometallics* **1986**, *5*, 609.

(26) Blomberg, M. R. A.; Siegbahn, P. E. M.; Nagashima, U.; Wennerberg, J. *J. Am. Chem. Soc.* **1991**, *113*, 424.

(27) Halle, L. F.; Crowe, W. E.; Armentrout, P. B.; Beauchamp, J. L. *Organometallics* **1984**, *3*, 1694.

(28) Burnier, R. C.; Byrd, G. D.; Freiser, B. S. *J. Am. Chem. Soc.* **1981**, *103*, 4360.

**Table 1.** Reaction Enthalpies and Average Kinetic Energy Releases from Experiment and Phase Space Theory

reaction	$-\Delta H^a$ (eV)	$\bar{E}_1$ (eV)	
		expt <sup>b</sup>	theory <sup>c</sup>
$\text{Fe}^+ + (\text{CH}_3)_2\text{CO} \rightarrow \text{FeC}_2\text{H}_6^+ + \text{CO}$	0.58	0.09	0.10
$\text{Fe}^+ + (\text{CH}_3)_2\text{CO} \rightarrow \text{FeCO}^+ + \text{C}_2\text{H}_6$	1.18	0.12	0.12
$\text{Co}^+ + (\text{CD}_3)_2\text{CO} \rightarrow \text{CoC}_2\text{D}_6^+ + \text{CO}$	1.02	0.12	0.12
$\text{Co}^+ + (\text{CD}_3)_2\text{CO} \rightarrow \text{CoCO}^+ + \text{C}_2\text{D}_6$	1.50	0.15	0.13
$\text{Ni}^+ + (\text{CH}_3)_2\text{CO} \rightarrow \text{NiC}_2\text{H}_6^+ + \text{CO}$	1.05	0.12	0.12
$\text{Ni}^+ + (\text{CH}_3)_2\text{CO} \rightarrow \text{NiCO}^+ + \text{C}_2\text{H}_6$	1.48	0.13	0.14

<sup>a</sup> Heats of reaction at 0 K, deuterium effects assumed to be negligible.  
<sup>b</sup>  $\bar{E}_1 \pm 0.005$  eV. <sup>c</sup> Statistical phase space theory described in the Appendix.

distributions.<sup>35</sup> The reported KERDs represent an average of several hundred scans repeated on at least two separate occasions.

Decomposition of the nascent  $\text{M}^+$ -acetone adduct in the second field-free region occurs for ions with lifetimes of about 5 to 15  $\mu\text{s}$ . It is possible the adducts are formed from both ground state and electronically excited state transition metal ions. Studies of state-selected  $\text{Fe}^+$ ,  $\text{Co}^+$ , and  $\text{Ni}^+$  reacting with propane show that the electronically excited metal ions react much more quickly than ground state ions,<sup>13,14</sup> decomposing prior to being mass selected. A similar increase in reactivity is expected for electronically excited  $\text{Fe}^+$ ,  $\text{Co}^+$ , and  $\text{Ni}^+$  reacting with acetone. In addition, the available energy for electronically excited metal ions reacting with acetone is greater than that for the ground state ion. Therefore, if initially excited state  $\text{M}^+$  ions produce products on the ground state surfaces, the energy partitioned into relative translational energy of the products should increase. Thus, KERDs for complexes formed from excited state ions are expected to be broader than those from ground state ions. Consequently, if a mixture of ground and excited state systems was fragmenting in the second field-free region, bimodal KERDs should result. No such effect was observed in any of the KERDs reported here, indicating that the contribution of electronic excited states is negligible. It should be mentioned, however, that the  $\text{Fe}^+$  (<sup>6</sup>D, 4s3d<sup>6</sup>) ground state is believed to efficiently cross to the  $\text{Fe}^+$  (<sup>4</sup>F, 3d<sup>7</sup>) first excited state when approaching the acetone ligand and entering the initial electrostatic well. This feature has been discussed previously in reactions of  $\text{Fe}^+$  with propane<sup>15</sup> and occurs because 3d<sup>n</sup> metal ions are much more strongly electrostatically bound to ligands than 4s3d<sup>n-1</sup> ions.

All chemicals were obtained commercially and were purified only by freeze-pump-thaw cycles to remove noncondensable gases.  $\text{Fe}(\text{CO})_5$  and  $\text{Co}(\text{CO})_3\text{NO}$  were obtained from Strem Chemical,  $\text{Ni}(\text{CO})_4$  from Alfa Inorganics, and acetone-*d*<sub>6</sub> (99.5 atom % D) from Stohler Isotope Chemicals.

## Results

KERDs for the metastable decomposition reactions of nascent adducts of  $\text{Fe}^+$ ,  $\text{Co}^+$ , and  $\text{Ni}^+$  with acetone were measured. Average kinetic energy releases,  $\bar{E}_1$ , obtained from experiment are given in Table 1. The KERDs for CO loss are shown in Figure 1 and those for  $\text{C}_2\text{H}_6$  loss in Figure 2. Note that for  $\text{Co}^+$ , deuterated acetone was used to avoid mass overlap between  $\text{Co}((\text{CH}_3)_2\text{CO})^+$  and  $\text{Co}(\text{CONO})^+$ , arising from the  $\text{Co}(\text{CO})_3\text{NO}$  precursor compound. While the KERD for  $\text{C}_2\text{H}_6$  loss from  $\text{Co}((\text{CH}_3)_2\text{CO})^+$  (a strong reaction channel with minimal

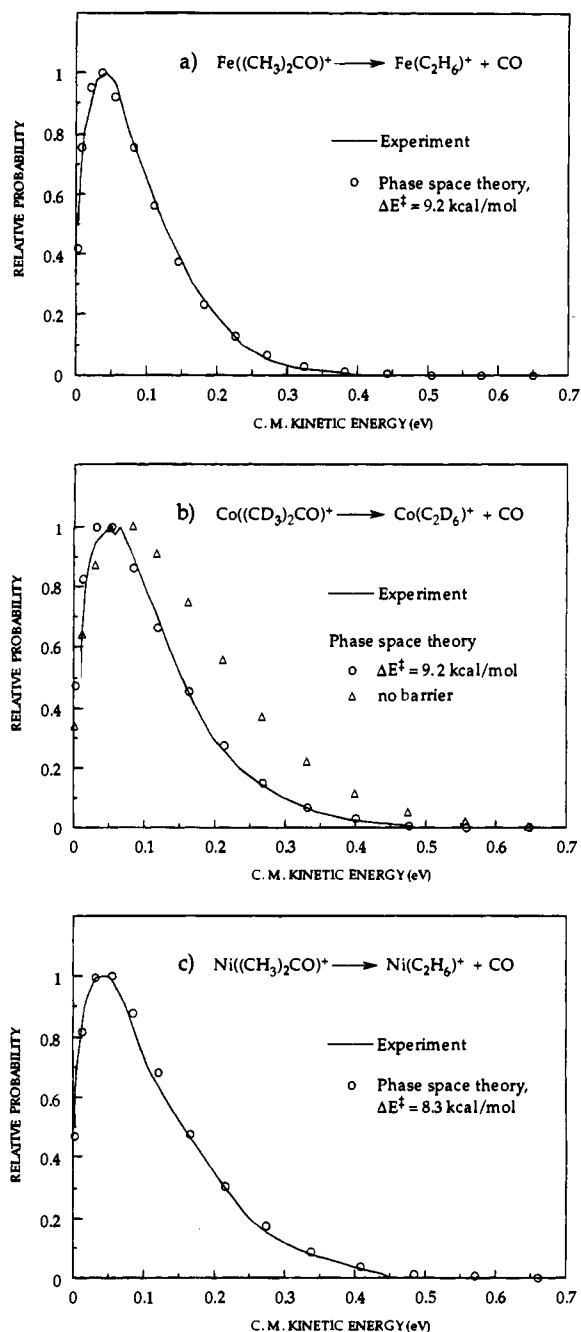


**Figure 1.** Experimental and theoretical kinetic energy release distributions for (a) loss of CO from  $\text{Fe}((\text{CH}_3)_2\text{CO})^+$ , (b) loss of CO from  $\text{Co}((\text{CD}_3)_2\text{CO})^+$ , and (c) loss of CO from  $\text{Ni}((\text{CH}_3)_2\text{CO})^+$ . Phase space theory calculations including the tight transition state are shown as open circles (O). In part (b) we show, for the  $\text{Co}^+$  ion, the same calculations with the tight TS removed ( $\Delta$ ). Similar results are obtained if the tight TS is removed in the  $\text{Fe}^+$  and  $\text{Ni}^+$  calculations.

interference due to NO loss from  $\text{Co}(\text{CONO})^+$ ) could be measured, interference from CO loss from  $\text{Co}(\text{CONO})^+$  prevented the measurement of the CO-loss KERD from  $\text{Co}((\text{CH}_3)_2\text{CO})^+$ . The KERDs for ethane loss from the deuterated and undeuterated  $\text{Co}^+$ -acetone adduct were compared. It was found that both KERDs could be matched by phase space theory assuming the same  $\Delta H_{\text{rxn}}$ . We expect that  $\Delta H_{\text{rxn}}$  for the CO-loss channel for both the deuterated and undeuterated systems should also be the same. This implies that the  $\text{Co}^+-\text{C}_2\text{H}_6$  and  $\text{Co}^+-\text{C}_2\text{D}_6$  bond energies are the same, which one would expect given the large electrostatic contribution to the bond.<sup>23</sup> Thus, no further distinction between the deuterated and undeuterated  $\text{Co}^+$ /acetone systems will be made.

(35) (a) Jarrold, M. F.; Illies, A. J.; Bowers, M. T. *Chem. Phys.* **1982**, 65, 19. (b) Kirchner, N. J.; Bowers, M. T. *J. Phys. Chem.* **1987**, 91, 2573.

(36) Schultz, R. H.; Armentrout, P. B. *J. Phys. Chem.* **1992**, 96, 1662.

(37) Haynes, C. L.; Fisher, E. R.; Armentrout, P. B. Work in progress.

(38) Schultz, R. H.; Crellin, K. C.; Armentrout, P. B. *J. Am. Chem. Soc.* **1991**, 113, 8590.

(39) Ricca, A.; Bauschlicher, C. W., Jr. *J. Phys. Chem.* **1994**, 98, 12899.  $D_0(\text{Fe}^+-\text{CO})$  in Table 2 is given relative to the  $\text{Fe}^+(4s3d^6, ^6D) + \text{CO}$  asymptote.

(40) Kahn, F. A.; Goebel, S.; Haynes, C. L.; Armentrout, P. B. Work in progress.

(41) Kahn, F. A.; Steele, D. A.; Armentrout, P. B. *J. Phys. Chem.* Submitted for publication.

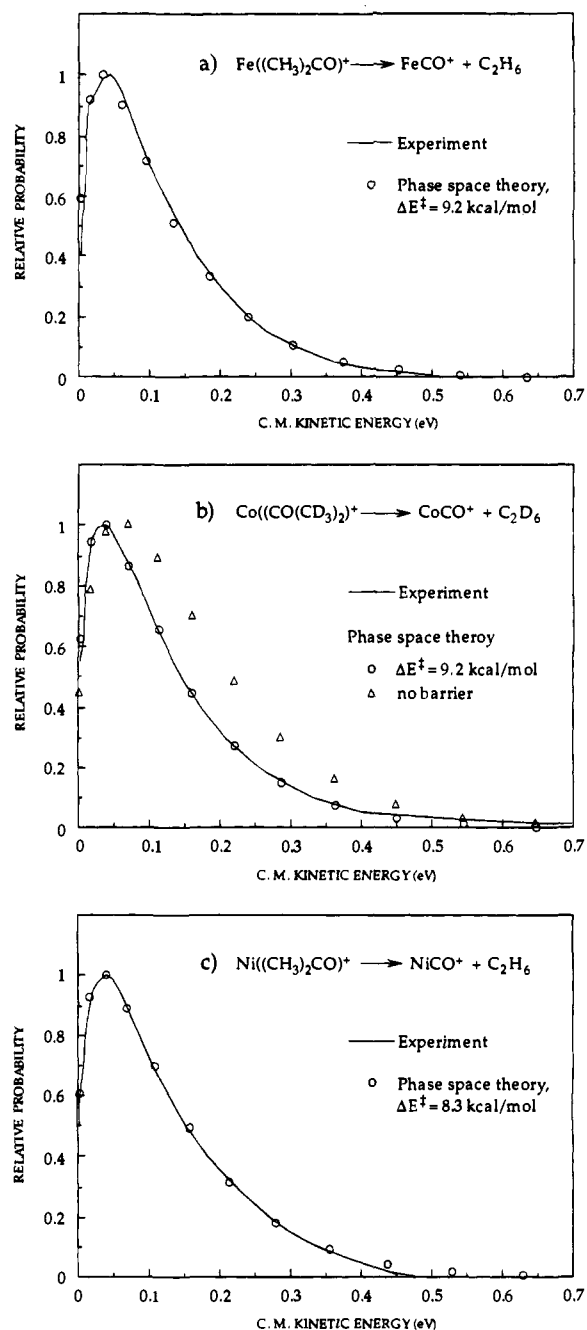


**Figure 2.** Experimental and theoretical kinetic energy release distributions for (a) loss of  $C_2H_6$  from  $Fe((CH_3)_2CO)^+$ , (b) loss of  $C_2D_6$  from  $Co((CO)(CD_3)_2)^+$ , and (c) loss of  $C_2H_6$  from  $Ni((CH_3)_2CO)^+$ . Phase space theory calculations including the tight transition state are shown as the open circles (O). In part (b) we show, for the  $Co^+$  ion, the same calculations with the tight TS removed ( $\Delta$ ). Similar results are obtained if the tight TS is removed in the  $Fe^+$  and  $Ni^+$  calculations.

In order to analyze the KERDs in Figures 1 and 2, it is useful to introduce the simplified reaction coordinate diagram given in Figure 3. In this diagram, only a single rate-limiting TS is shown since this TS will dominate the kinetics and dynamics of the reaction being studied. The nature of this TS will be discussed shortly. Based on the schematic reaction coordinate diagram shown in Figure 3, the only two important variables in matching experiment with theory are the reaction exothermicity ( $\Delta H_{rxn}$ ) and the energy of the rate-limiting, tight TS relative to the energy of the reactants ( $\Delta E^\ddagger$ ). While the KERDs are sensitive to the energy of the tight TS structure, the properties of the TS such as rotational constants and vibrational frequencies may be varied over a fairly wide range of reasonable values

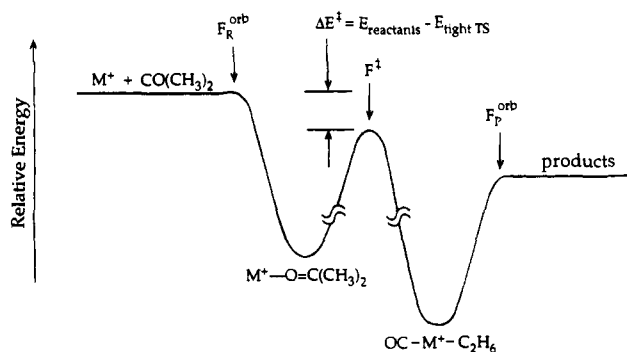


**Figure 3.** A schematic reaction coordinate diagram for  $M^+$  reacting with acetone.  $F_R^{orb}$ ,  $F^\ddagger$ , and  $F_P^{orb}$  are the fluxes through the reactant orbiting transition state, the rate-determining, tight transition state, and the product orbiting transition state, respectively. There are other transition states along the reaction coordinate, but these are assumed to have little effect on the KERDs for these reactions.

without changing the KERD significantly. Thus, given the reaction exothermicity, we can determine  $\Delta E^\ddagger$ . Figures 1 and 2 show experimental KERDs for CO and  $C_2H_6$  loss along with the KERDs calculated with phase space theory. In the theoretical KERDs shown, it was assumed that the rate-limiting transition state corresponds to C-C bond activation.

Temperature-dependent equilibria experiments have been used to measure a reliable value for the  $Co^+-C_2H_6$  bond energy of  $28.0 \pm 1.6$  kcal/mol.<sup>22</sup> Using this value, we can calculate  $\Delta H_{rxn}$  for  $Co^+$  reacting with acetone to eliminate CO. Given  $\Delta H_{rxn}$ ,  $\Delta E^\ddagger$  was determined to be  $9.2 \pm 2$  kcal/mol by modeling the KERD for CO elimination using phase space theory (Figure 1b). The effect of the rate-limiting TS on the average kinetic energy released can be seen in Figures 1b and 2b. The KERDs predicted by phase space theory including the rate-limiting TS (with  $\Delta E^\ddagger = 9.2$  kcal/mol) and leaving out the rate-limiting TS (which is equivalent to setting  $\Delta E^\ddagger$  to be very large) are shown. Fitting the experimental CO-loss KERD with theory by leaving out the rate-limiting TS and varying  $\Delta H_{rxn}$  leads to a  $Co^+-C_2H_6$  bond energy of 17.2 kcal/mol, which is unreasonably low. Thus, the rate-limiting TS must be included in the theoretical model for  $Co^+$  reacting with acetone.

Using  $\Delta E^\ddagger = 9.2$  kcal/mol to model the KERD for  $C_2H_6$  loss, the  $Co^+-CO$  bond energy was determined to be  $39.1 \pm 3$  kcal/mol (Figure 2b). This result, along with *ab initio* calculations, was used to determine relative  $Fe^+-CO$  and  $Ni^+-CO$  bond energies. Barnes *et al.* have performed thorough *ab initio* calculations on first- and second-row transition-metal mono- and dicarbonyl positive ions.<sup>33</sup> They find that  $D_0^0(Fe^+-CO) = 30.3$  kcal/mol,  $D_0^0(Co^+-CO) = 37.3$  kcal/mol, and  $D_0^0(Ni^+-CO) = 36.7$  kcal/mol or relative bond energies of 1.00/1.23/1.21 for  $Fe^+/Co^+/Ni^+$ . The values of these bond energies relative to each other are believed to be quite good. Thus, if these same ratios of bond strengths are used with our experimental value for the  $Co^+-CO$  bond strength we obtain  $31.8 \pm 3$  and  $38.5 \pm 3$  kcal/mol for  $Fe^+-CO$  and  $Ni^+-CO$ , respectively. Use of  $D_0^0(Fe^+-CO) = 31.8$  and  $D_0^0(Ni^+-CO) = 38.5$  kcal/mol allowed determination of  $\Delta H_{rxn}$  for these systems. The KERDs for the  $C_2H_6$ -loss channels for  $Fe^+$  and  $Ni^+$  reacting with acetone were modeled and  $\Delta E^\ddagger$  for the rate-limiting transition states were found to be  $9.2 \pm 2$  and  $8.3 \pm 2$  kcal/mol for  $Fe^+$  and  $Ni^+$ , respectively. These values of  $\Delta E^\ddagger$  were then used to model the KERDs for CO loss from  $Fe^+$  and  $Ni^+$ -acetone. By this method,  $Fe^+-C_2H_6$  and  $Ni^+-C_2H_6$  bond energies were determined to be  $17.9 \pm 3$  and  $28.7 \pm 3$  kcal/mol, respectively. A summary of the bond energies from

**Table 2.** Comparison of Bond Energies (in kcal/mol)

	M	this study <sup>a</sup>	ion beam	theory
$D_0^{\ddagger}(M^+-C_2H_6)$	Fe	$17.9 \pm 3^b$	$15.3 \pm 1.4^c$	$26.4 \pm 2^f$
	Co	$28.0 \pm 1.6^d$	$24.0 \pm 1.2^e$	
	Ni	$28.7 \pm 3^b$		
$D_0^{\ddagger}(M^+-CO)$	Fe	$31.8 \pm 3^g$	$31.3 \pm 1.8^h$	$30.3^i$ (33.1) <sup>j</sup>
	Co	$39.1 \pm 3^b$	$41.5 \pm 1.6^k$	$37.3^l$
	Ni	$38.5 \pm 3^g$	$41.7 \pm 2.5^l$	$36.7^i$

<sup>a</sup> The error bars, with the exception of that for  $D_0^{\ddagger}(Co^+-C_2H_6)$ , include both uncertainty in the measurement of  $D_0^{\ddagger}(Co^+-C_2H_6)$  (ref 22) and the KERDs as well as uncertainty in the parameters used in the phase space calculations. <sup>b</sup> Bond energy determined by modeling KERRD. <sup>c</sup> Reference 36. <sup>d</sup> From equilibrium experiments, ref 22. <sup>e</sup> Reference 37. <sup>f</sup> Reference 23. <sup>g</sup> Determined from  $D_0^{\ddagger}(Co^+-CO)$  in conjunction with  $D_0^{\ddagger}(M^+-CO)$  from theory (see text). <sup>h</sup> Reference 38. <sup>i</sup> Reference 33. <sup>j</sup> Reference 39. <sup>k</sup> Reference 40. <sup>l</sup> Reference 41.

**Table 3.**  $\Delta E^{\ddagger}$  (in kcal/mol) for  $M^+$  Inserting into a C-C Bond of Acetone and a C-H Bond of Propane

M	$\Delta E_{C-C}^{\ddagger}(\text{acetone})^a$	$\Delta E_{C-H}^{\ddagger}(\text{propane})^b$
Fe	$9.2 \pm 2$ ( $14.9 \pm 2$ ) <sup>c</sup>	$1.7 \pm 0.7$ ( $7.4 \pm 0.7$ ) <sup>c</sup>
Co	$9.2 \pm 2$	$2.5 \pm 0.7$
Ni	$8.3 \pm 2$	$2.3 \pm 0.7$

<sup>a</sup> The error bars include uncertainty in the measurement of  $D_0^{\ddagger}(Co^+-C_2H_6)$  (ref 22) and the KERDs as well as the uncertainty in the parameters used in the phase space calculations. <sup>b</sup> Reference 15. <sup>c</sup> Relative to the  $Fe^+(^4F, 3d^7)$  asymptotic energy.

this study in comparison to literature values is shown in Table 2, and the values of  $\Delta E^{\ddagger}$  are given in Table 3.

## Discussion

**Rate-Limiting Transition State.** There are two pieces of experimental evidence that suggest there is a tight transition state that is rate limiting along the reaction coordinate for  $Fe^+$ ,  $Co^+$ , and  $Ni^+$  reacting with acetone. First, Halle *et al.* have measured cross sections for the  $Co^+$  + acetone reaction.<sup>27</sup> Their results indicate that even though both  $C_2H_6$  and  $CO$  loss channels are exothermic, the total reaction efficiency is only 29%.

Second, using reasonable  $M^+-C_2H_6$  and  $M^+-CO$  bond energies, the experimental KERDs for  $CO$  and  $C_2H_6$  loss from acetone reacting with all three metal ions can only be matched with statistical phase space theory if a tight TS is included in the model. Failure to use a tight TS leads to prediction of KERDs much broader than experiment because the tight TS imposes angular momentum restrictions on the reaction.<sup>15</sup> Reactant collision complexes with high angular momenta are effectively blocked from going on to products because the barrier in the effective PES for the tight TS rises more quickly with increasing angular momentum than the barrier for the reactant orbiting TS. As a result, high angular momentum collision complexes dissociate back to reactants and the average kinetic energy released to the products is reduced.

There are several possibilities for this rate-limiting TS, with leading candidates being initial C-C bond activation and C-C bond coupling as exemplified in Scheme 1 and in the schematic PES for  $Co^+$  reacting with acetone (Figure 4). We will discuss these possibilities in order. First consider the initial C-C bond activation TS. Preliminary *ab initio* calculations indicate that the  $Co^+$  + acetone complex has a binding energy of  $52 \pm 3$  kcal/mol.<sup>29</sup> This result is in good agreement with the estimate of 51 kcal/mol by Halle *et al.*<sup>27</sup> The structure of this complex has the metal ion bound to the oxygen atom in a linear  $M^+-O-C$  configuration. Before C-C bond activation can be initiated, the metal ion has to migrate and become centered on one of the C-C bonds of acetone. In propane, the PES in the

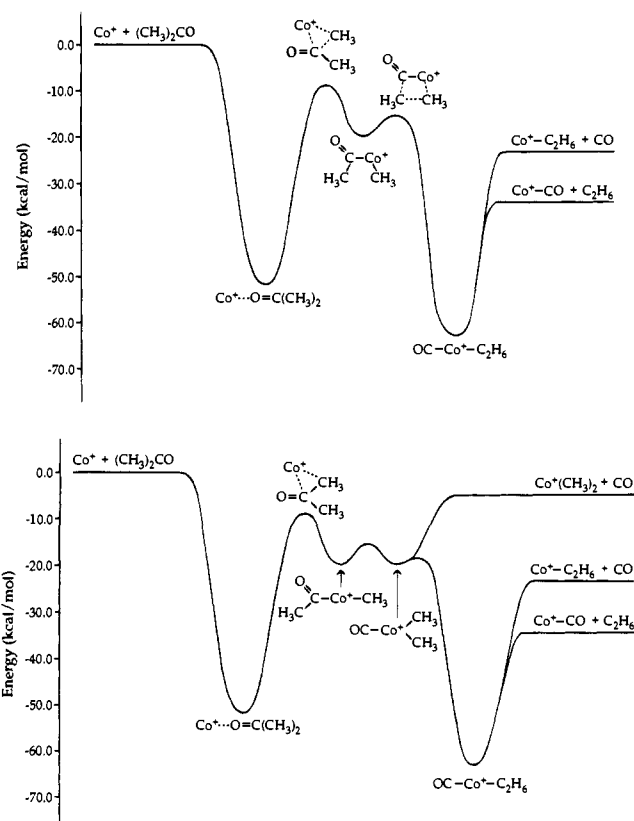


**Figure 4.** Schematic reaction coordinate diagram for  $Co^+$  reacting with acetone assuming C-C bond activation is rate limiting (see text). The top diagram assumes the only important intermediate is  $(CH_3CO)M^+-CH_3$  while the bottom diagram assumes a  $OC-M^+(CH_3)_2$  species is also involved. The asymptotic energies are all well-known, and excellent estimates are available for the  $M^+-OC(CH_3)_2$  and  $OC-M^+-C_2H_6$  species. The initial C-C bond activation transition state was taken to be rate limiting (see text) and its energy set from the value of  $\Delta E^{\ddagger} = 9 \pm 1$  kcal/mol determined here. The energies of the  $(CH_3CO)M^+-CH_3$  and  $OC-M^+(CH_3)_2$  intermediates are only qualitatively estimated.

region of the  $M^+ \cdot C_3H_8$  complex is quite flat, all configurations have essentially the same energy, and no such reorientation is required. Since the  $M^+$  ions are "electrostatically" bound to acetone, approximately 20 kcal/mol more strongly than to propane, due to the directional forces of the dipole moment, this reorientation energy is substantial, possibly on the order of 20 kcal/mol and certainly greater than 10 kcal/mol. Suppose that in fact the reorientation energy of  $M^+$  in acetone was the maximum value of 20 kcal/mol, and suppose further that the same amount of energy was required to activate the C-C bond in acetone as in propane. Under these circumstances, the resulting C-C bond activation TS would lie above the  $M^+$ /acetone asymptotic energy (as it does in propane) and consequently no reaction could occur.<sup>42</sup> Since reaction does occur, this reasoning needs to be modified. Two effects can lower the TS energy. First, the C-C bond in acetone is 6 kcal/mol weaker than the C-C bond in propane. Consequently, a

(42) In reactions of  $M^+$  ions with propane, no evidence for C-C bond activation was observed (ref 15). Experiment (ref 24) suggests the C-C bond activation transition state in  $Fe^+/C_3H_8$  is  $\sim 8$  kcal/mol above the C-H transition state. Theory (refs 25 and 26) suggests C-C bond activation transition states are substantially higher in energy than C-H transition states due to orbital realignment effects. Since the C-H bond activation transition state for  $M^+$ /propane is only 2 to 3 kcal/mol below the  $M^+$ /propane asymptotic energy, the C-C bond activation transition state is most likely at least 5 kcal/mol above this energy. We can say with some certainty that failure to observe C-C bond activation in propane strongly supports the fact that the transition state must be above the  $M^+$ /propane asymptotic energy.

lowering of the insertion TS by  $\sim 6$  kcal/mol relative to propane is not unreasonable. Second, the reorientation energy may be less than 20 kcal/mol, say 10 or 15 kcal/mol. This would lower the TS energy proportionately. These two effects would then place the C–C bond activation TS  $10 \pm 5$  kcal/mol below the  $M^+$ /acetone asymptote in good agreement with our determination of  $9 \pm 3$  kcal/mol for  $\Delta E^\ddagger$ . Consequently, initial C–C bond activation is an excellent candidate for the rate-limiting TS.

Next, let us consider the C–C bond coupling transition state. From the perspective of the reverse reaction, this transition state arises from insertion of the  $OC-M^+$  moiety into the C–C bond of  $C_2H_6$  to form either  $OC-M^+(CH_3)_2$  or  $(CH_3CO)M^+-CH_3$  (see Figure 4). The energy of the  $OC-M^+-C_2H_6$  complex can be accurately estimated from known thermochemical data to be 60 kcal/mol below the  $M^+$ /acetone asymptote.<sup>43</sup> In this instance there is no reorientation energy to consider since the metal ion is centered on the  $C_2H_6$  axis in the  $OC-M^+-C_2H_6$  complex. If the C–C bond activation energy is the same in ethane as it is in propane, it would occur  $\sim 38$  kcal/mol above the energy minimum of the  $OC-M^+-C_2H_6$  potential well, or  $\sim 22$  kcal/mol below the  $M^+$ /acetone asymptote.<sup>44</sup> How the CO ligand might affect the metal ion's ability to insert into  $\sigma$  bonds is uncertain,<sup>45</sup> but the insertion products are expected to be similar in energy whether  $M^+$  is inserting into acetone or  $OC-M^+$  is inserting into  $C_2H_6$  so the effects of the insertion products on the insertion transition state energies should be comparable for both processes. As a consequence, it appears the C–C coupling transition state (to form  $OC-M^+(CH_3)_2$ ) occurs  $\sim 10$  kcal/mol lower in energy than the initial C–C insertion transition state and hence is probably not rate limiting.

It is possible (probable?) that the  $(CH_3CO)M^+-CH_3$  intermediate is directly formed from the insertion of  $OC-M^+$  into the C–C bond of  $C_2H_6$ . In this instance the intermediate would be identical with that formed from C–C bond insertion of  $M^+$  into acetone. Looked at from the perspective of this  $(CH_3CO)M^+-CH_3$  intermediate, the issue is whether it is easier to rearrange to form  $M^+-OC(CH_3)_2$  or  $OC-M^+-C_2H_6$ ? Since  $OC-M^+-C_2H_6$  is 8 kcal/mol more stable than  $M^+-OC(CH_3)_2$ , this suggests the TS leading to this product is lower in energy than the TS leading to  $M^+-OC(CH_3)_2$ . In addition, it appears the TS forming  $OC-M^+-C_2H_6$  is less strained than the one that leads to  $M^+-OC(CH_3)_2$ , which should again lower its energy (see Figure 4a). Consequently it appears most likely that the C–C insertion TS is rate limiting.

The qualitative, and sometimes semiquantitative, arguments made above favor the initial C–C insertion transition state as rate limiting. An attempt has been made to consider the effect of the CO group on the various rearrangements as well as take advantage of our more extensive knowledge of the propane system. At present, we are pursuing high-level, electronic-

(43) This value can be determined from the exothermicities of the reaction channels and the  $Co^+-C_2H_6$  and  $Co^+-CO$  bond energies minus  $\sim 2$  kcal/mol because the second ligand is less strongly bound (for example, see ref 22 for the first and second  $C_2H_6$  binding energies and ref 40 for the first and second CO binding energies).

(44) The binding energy of  $Co^+$  to  $C_3H_8$  is  $\sim 32$  kcal/mol (see Table 4). The C–H bond insertion transition state for  $Co^+$  in propane is 2.5 kcal/mol below the  $Co^+$ /propane asymptotic energy, or  $\sim 30$  kcal/mol above the minimum in the  $Co^+-C_3H_8$  complex well. If the C–C bond activation transition state is  $\sim 8$  kcal/mol higher in energy than the C–H transition state, then it should occur  $\sim 38$  kcal/mol above the minimum energy of association complex.

(45) A study of the effect a CO ligand has on  $Fe^+$  activating the D–D bond in deuterium has recently been published: Tjetta, B. L.; Armentrout, P. B. *J. Am. Chem. Soc.* **1995**, *117*, 5531.

**Table 4.** Experimental and Theoretical Bond Energies (in kcal/mol)

$D_0^\ddagger$	expt		
	equilibrium measurements <sup>a</sup>	ion beam	theory <sup>b</sup>
$Co^+-CH_4$	$22.9 \pm 0.7$	$21.4 \pm 1.4^c$	$22.7 \pm 2$
$Co^+-C_2H_6$	$28.0 \pm 1.6$	$24.0 \pm 1.2^d$	$26.4 \pm 2$
$Co^+-C_3H_8$		$30.9 \pm 1.4^d$	$30.8 \pm 2$

<sup>a</sup> Reference 22. <sup>b</sup> Reference 23. <sup>c</sup> Reference 60. <sup>d</sup> Reference 37.

structure calculations<sup>46</sup> on the  $M^+$ /acetone potential energy surfaces and depending on the outcome of these calculations some of the arguments made above may have to be modified.

**Energy of the Rate-Limiting Transition State for  $Co^+$ .** To determine the energy of the rate limiting transition state for  $Co^+$  reacting with acetone, the  $Co^+-C_2H_6$  bond energy was taken from the literature. We chose the value  $D_0^\ddagger(Co^+-C_2H_6) = 28.0 \pm 1.6$  kcal/mol both because of the inherent accuracy of the equilibrium method used to determine this number<sup>22</sup> and because it was in excellent agreement with theoretical calculations on the trend observed in  $Co^+-CH_4$ ,  $Co^+-C_2H_6$ , and  $Co^+-C_3H_8$  bond energies (see Table 4). The other experimental value of the  $Co^+-C_2H_6$  bond energy of 24.0 kcal/mol, measured in the ion beam experiments,<sup>37</sup> seems too low with respect to the theoretical value of 26.4 kcal/mol<sup>23</sup> and with respect to the theoretical and experimental trends in bond energies for  $Co^+-CH_4$ ,  $Co^+-C_2H_6$ , and  $Co^+-C_3H_8$ . The CO-loss KERD for  $Co^+$  + acetone was modeled using  $D_0^\ddagger(Co^+-C_2H_6) = 28.0$  kcal/mol. We obtained  $\Delta E^\ddagger = 9.2$  kcal/mol, which in turn was used to determine a  $Co^+-CO$  bond energy of 39.1 kcal/mol. This bond energy for  $Co^+-CO$  is in good agreement with the theoretical value of 37.3 kcal/mol.<sup>33</sup> When  $D_0^\ddagger(Co^+-C_2H_6) = 24.0$  kcal/mol is used to model the KERD,  $\Delta E^\ddagger$  must be increased to 15.0 kcal/mol, giving a  $Co^+-CO$  bond energy of 35.6 kcal/mol, which is an unreasonably low value with respect to both the theoretical and the other experimental values.

**$M^+-CO$  Bond Energies.** As noted above, from analysis of the KERD we determined  $D_0^\ddagger(Co^+-CO) = 39.1 \pm 3$  kcal/mol. High-level theory<sup>33</sup> yields a value of 37.3 kcal/mol for this bond energy. Theoretical estimates of binding energies are almost always lower than experiment. In the present instance, Barnes *et al.*<sup>33</sup> and Ricca *et al.*<sup>39</sup> state that their numbers are low by 2 to 3 kcal/mol, indicating excellent agreement with our experimental number. In addition, their calculations should give very accurate relative bond strengths as the metal ion is varied across the row, especially for adjacent ions like  $Fe^+$ ,  $Co^+$ , and  $Ni^+$  where orbital size and energies are similar. Consequently, our use of their relative bond strengths to scale our experimental value of  $D_0^\ddagger(Co^+-CO)$  should yield very accurate values of  $D_0^\ddagger(Fe^+-CO)$  and  $D_0^\ddagger(Ni^+-CO)$ .

Our values for these bond energies are in relatively good agreement with ion beam studies by Armentrout and co-workers, especially for  $Fe^+-CO$ . While the ion beam results for  $Co^+-CO$ <sup>40</sup> and  $Ni^+-CO$ <sup>41</sup> are about 3 kcal/mol higher than our numbers, they do fall within the quoted experimental errors of both measurements.

Theoretical and experimental values for the  $M^+-CO$  bond energies for  $M = Fe, Co,$  and  $Ni$  (Table 2) indicate that the  $Fe^+-CO$  bond energy is significantly lower than the  $Co^+-CO$  and  $Ni^+-CO$  bond energies. This reduction is due to the different electron configurations of the metal ions. While  $Co^+$  has a ( $3d^8, ^3F$ ) ground state and  $Ni^+$  has a ( $3d^9, ^2D$ ) ground

(46) Perry, J. K.; van Koppen, P. A. M.; Carpenter, C. J.; Bowers, M. T. Work in progress.

state,  $\text{Fe}^+$  has a ( $3d^6 4s^1$ ,  ${}^6D$ ) ground state.<sup>47</sup> Barnes *et al.*<sup>33</sup> considered both the  ${}^6\Pi$  and  ${}^4\Sigma^-$  states of  $\text{FeCO}^+$  and found the  ${}^6\Pi$  state to be weakly bound with respect to ground state  $\text{Fe}^+$  ( $4s3d^6$ ,  ${}^6D$ ) + CO due to the presence of the repulsive  $4s$  electron. However, the  ${}^4\Sigma^-$  state was found to be strongly bound relative to the  $\text{Fe}^+$  ( $3d^7$ ,  ${}^4F$ ) + CO first excited state. Consequently,  $\text{FeCO}^+$  produced in the reaction of  $\text{Fe}^+$  and acetone is in the  ${}^4\Sigma^-$  state. The binding energy reported for  $\text{FeCO}^+$  is relative to the  $\text{Fe}^+$  ( $4s3d^6$ ,  ${}^6D$ ) + CO asymptote. The splitting between the ground and first excited state of  $\text{Fe}^+$  is 5.7 kcal/mol.<sup>47a</sup> Hence, the  $\text{Fe}^+$ -CO bond energy with respect to the  $3d^7$  state of  $\text{Fe}^+$  is 37.5 kcal/mol, which is in the same range as the  $\text{Co}^+$ - and  $\text{Ni}^+$ -CO bond energies.

**$M^+$ - $C_2H_6$  Bond Energies.** The bond energy for  $\text{Fe}^+$ - $C_2H_6$  of  $17.9 \pm 3$  kcal/mol (relative to the ground state  $\text{Fe}^+$  ( $4s3d^6$ ,  ${}^6D$ ) +  $C_2H_6$  asymptote) is substantially smaller than  $D_0(\text{Co}^+-C_2H_6) = 28.0 \pm 3$  and  $D_0(\text{Ni}^+-C_2H_6) = 28.7 \pm 3$  kcal/mol (with respect to ground state  $\text{Co}^+$  ( $3d^8$ ,  ${}^3F$ ) and  $\text{Ni}^+$  ( $3d^9$ ,  ${}^2D$ ) +  $C_2H_6$  asymptotes, respectively). The  $\text{Fe}^+$ - $C_2H_6$  bond energy is low for the same reason the  $\text{Fe}^+$ -CO bond energy is low (again because of the repulsive  $4s$  electron in the ground electronic configuration of  $\text{Fe}^+$ ) and is in reasonable agreement with the value of  $15.3 \pm 1.4$  kcal/mol obtained using ion beam methods.<sup>36</sup> Theoretical studies on  $\text{Co}^+-C_2H_6$  have provided insight into the bonding of these complexes. Perry *et al.*<sup>23</sup> found the lowest energy structure of this complex to be an  $\eta^3 C_s$  configuration with a singly occupied  $d_{\sigma}$ -like orbital on cobalt directed to an in-plane C-H bond of ethane and a singly occupied  $d_{\pi}$ -like orbital directed to two out-of-plane C-H bonds on the other carbon of ethane. There is electron donation from the ethane into these orbitals, as well as to the  $4s$  orbital on the metal. Unlike the  $M^+$ -CO bond, no back bonding is observed for  $\text{Co}^+-C_2H_6$ . This gives rise to the lower  $M^+-C_2H_6$  bond energies relative to  $M^+$ -CO bond energies for  $\text{Fe}^+$ ,  $\text{Co}^+$ , and  $\text{Ni}^+$ . The lack of  $\pi$  back-donation in  $M^+-C_2H_6$  may also explain why the  $\text{Co}^+$ - and  $\text{Ni}^+-C_2H_6$  bond energies are similar.

**Energy of the Rate-Limiting Transition State for  $\text{Fe}^+$  and  $\text{Ni}^+$ .** The rate-limiting TS was found to lie 9.2 kcal/mol below the energy of the  $\text{Co}^+$  ( ${}^3F$ ,  $3d^8$ ) + acetone reactants and 8.3 kcal/mol below the energy of the  $\text{Ni}^+$  ( ${}^2D$ ,  $3d^9$ ) + acetone reactants. On the other hand, the TS for ground state  $\text{Fe}^+$  ( ${}^6D$ ,  $4s3d^6$ ) reacting with acetone lies 9.2 kcal/mol below the asymptotic energy of the reactants, placing it 14.9 kcal/mol below the  $\text{Fe}^+$  ( ${}^4F$ ,  $3d^7$ ) + acetone asymptote. If the rate-limiting TS is in fact C-C bond activation, this discrepancy would be consistent with the donation from the  $\sigma$  orbital into the empty  $4s$  orbital on the metal ion that is involved in  $\sigma$  bond activation.<sup>6</sup> Insertion is easiest for transition metals where the  $4s$  orbital is most accessible. Consequently, the  $sd$  hybridization necessary to form a single metal-alkyl bond is easiest for  $\text{Fe}^+$ <sup>48</sup> since the promotion energy including  $d-d$  and  $s-d$  exchange energy is the smallest for  $\text{Fe}^+$ <sup>49</sup> (note that the  $4s$  orbital of  $\text{Fe}^+$  may actually be lower in energy than the  $3d$  orbitals<sup>47</sup>). As a result,  $\text{Fe}^+$  forms the strongest metal-alkyl bonds of the three metal ions.<sup>50</sup>

These results are consistent with the  $M^+/C_3H_8$  system<sup>15</sup> where the C-H bond activation barrier was also found to be

(47) (a) Moore, C. E. *Atomic Energy Levels*; U.S. National Bureau of Standards: Washington, DC, 1952; Circ. 467. (b) Sugar, J.; Corliss, C. J. *Phys. Chem. Ref. Data* **1981**, *10*, 197. (c) Sugar, J.; Corliss, C. J. *Phys. Chem. Ref. Data* **1981**, *10*, 1097. (d) Sugar, J.; Corliss, C. J. *Phys. Chem. Ref. Data* **1982**, *11*, 135.

(48) Perry, J. K. Ph.D. Thesis, California Institute of Technology, 1994.

(49) Armentrout, P. B.; Kickel, B. L. In *Organometallic Ion Chemistry*; Freiser, B. S., Ed.; Kluwer Academic Publishers: The Netherlands, in press.

(50) Armentrout, P. B.; Clemmer, D. E. In *Energetics of Organometallic Species*; Simoes, J. A. M., Ed.; Kluwer Academic Publishers: The Netherlands, 1992; pp 321-356.

significantly lower for  $\text{Fe}^+$  than for  $\text{Co}^+$  and  $\text{Ni}^+$  reacting with propane (relative to the  $M^+(d^n)$  asymptote; see Table 3). The C-H bond activation TS was found to be  $1.7 \pm 0.7$ ,  $2.5 \pm 0.7$ , and  $2.3 \pm 0.7$  kcal/mol below the energy of the ground state  $M^+$  + propane reactants for  $M = \text{Fe}$ ,  $\text{Co}$ , and  $\text{Ni}$ , respectively, and 7.4 kcal/mol below the  $\text{Fe}^+$  ( ${}^4F$ ,  $3d^7$ ) + propane asymptotic energy.

**Energetics for C-C and C-H Bond Activation.** If the rate limiting TS in the acetone reactions is due to C-C bond activation, we can use  $\Delta E^\ddagger$  to determine the C-C bond activation energy for cobalt ion. Using  $\Delta E^\ddagger = 9.2$  kcal/mol for the position of the C-C bond activation transition state and the binding energy of 52 kcal/mol for the  $\text{Co}^+$ -acetone adduct,<sup>29</sup> we obtain a C-C bond activation energy of about 43 kcal/mol. However, in order to compare with propane, as we discussed in the section on rate-limiting transition states, this value should be modified due to the 6 kcal/mol weaker C-C bond in acetone, relative to propane and the  $15 \pm 5$  kcal/mol reorientation energy. Consequently, the analogous C-C bond activation energy in propane should be  $34 \pm 5$  kcal/mol. From our previous studies on  $\text{Co}^+$  + propane,  $D_0(\text{Co}^+-C_3H_8) = 30.8$  kcal/mol<sup>23</sup> and  $\Delta E_{C-H}^\ddagger = 2.5$  kcal/mol,<sup>15</sup> indicating that approximately 28 kcal/mol is required to activate a C-H bond. Thus, the difference between C-C and C-H bond activation is on the order of  $6 \pm 5$  kcal/mol. This result is in good agreement with threshold collisional activation studies of  $\text{Fe}^+-C_3H_8$  which show that C-C bond activation takes  $\sim 8$  kcal/mol more energy than C-H bond activation.<sup>24</sup> It is also consistent with theoretical studies by Low and Goddard, who determined the transition state for C-C coupling to eliminate ethane to be 10 kcal/mol higher in energy than the transition state for C-H coupling to eliminate methane from the corresponding Pt and Pd complexes.<sup>25</sup> Similarly, Blomberg *et al.* found a difference of  $\sim 20$  kcal/mol for  $\text{Fe}$ ,  $\text{Co}$ , and  $\text{Ni}$  inserting into a C-H bond of methane relative to a C-C bond of ethane.<sup>26</sup> It is more difficult for  $M^+$  to insert into a C-C bond than a C-H bond due to the directionality of the  $sp^3$  hybrid orbital on carbon versus the spherical symmetry of the  $s$  orbital on hydrogen. Carbon has to reorient its  $sp^3$  (or  $sp^2$ ) orbitals while breaking a C-C bond in order to subsequently form a bond with the metal ion.

**$M^+ \cdot C_2H_6$  Versus  $M(\text{CH}_3)_2^+$  Product Ion.** There are two possibilities for the structure of the  $\text{MC}_2\text{H}_6^+$  products: an ethane adduct,  $M^+ \cdot C_2H_6$ , or a dimethyl complex,  $M(\text{CH}_3)_2^+$ . The CO-loss KERD from  $\text{Co}^+$ -acetone had been previously modeled using phase space theory, leaving out the rate-limiting TS and assuming only the dimethyl product is formed.<sup>21</sup> This resulted in a value for  $D_0(\text{Co}^+-\text{(CH}_3)_2)$  of 105 kcal/mol, a bond energy that is unreasonably high considering that theoretical calculations put the value at only 87.7 kcal/mol.<sup>51</sup> In addition, experimental evidence indicates this value is too high. A plot of bond energy versus  $s^1d^{n-1}$  promotion energy gives a straight line for first row metal ions and the intercept corresponds to the intrinsic  $M^+-\text{(CH}_3)_2$  binding energy. Such a plot indicates  $D_0(\text{Co}^+-\text{(CH}_3)_2) = 95$  kcal/mol.<sup>52</sup> Modeling the CO-loss KERD using phase space theory including the barrier for the rate-limiting TS and assuming only the dimethyl product is formed yields a value for  $D_0(\text{Co}^+-\text{(CH}_3)_2)$  of 113.3 kcal/mol, a value even more unreasonable than  $D_0(\text{Co}^+-\text{(CH}_3)_2) = 105$  kcal/mol determined using unrestricted phase space theory.

The possibility of producing only the  $M^+ \cdot C_2H_6$  adduct or a mixture of the two species needs to be considered. For  $\text{Co}^+$

(51) Rosi, M.; Bauschlicher, C. W., Jr.; Langhoff, S. R.; Parridge, H. J. *Phys. Chem.* **1990**, *94*, 8656.

(52) Armentrout, P. B. In *Bonding Energetics in Organometallic Compounds*; Marks, T. J., Ed.; ACS Symposium Series 428; American Chemical Society: Washington, DC, 1990; pp 18-33.

and  $\text{Ni}^+$  the reaction to form the ethane adduct is about 25 kcal/mol more exothermic than the reaction to form the dimethyl product, which is nearly thermoneutral.<sup>53</sup> As a consequence, the average kinetic energy released would be much smaller for the dimethyl product than it would be for the ethane adduct. Leaving out the rate-limiting TS, the experimental KERD can be matched assuming a mixture of the two isomers is formed. However, modeling the  $\text{C}_2\text{H}_6$ -loss KERDs (leaving out the rate-limiting TS) gives unreasonably low  $\text{M}^+-\text{CO}$  bond energies (about 50% too low) indicating this model is incorrect for these systems.<sup>54</sup> When the tight TS is included in the phase space theory to model the CO-loss KERDs, a maximum contribution of 10% of the  $\text{M}(\text{CH}_3)_2^+$  structure could be accommodated in the  $\text{Co}^+$  and  $\text{Ni}^+$  systems. Above a 10%  $\text{M}(\text{CH}_3)_2^+$  contribution, significant deviation between the theoretical and experimental KERDs was observed. The theoretical KERDs shown in Figure 1 assume only the  $\text{M}^+\cdot\text{C}_2\text{H}_6$  adduct is formed.

The  $\text{Fe}^+$ /acetone system is somewhat different than the  $\text{Co}^+$  and  $\text{Ni}^+$  systems. While  $\text{Fe}^+(\text{CH}_3)_2$  formation is still approximately thermoneutral,<sup>53</sup> the formation of  $\text{Fe}^+\cdot\text{C}_2\text{H}_6$  is only 13.4 kcal/mol exothermic. As a consequence there is a greater possibility for the formation of  $\text{Fe}(\text{CH}_3)_2^+$  than there is for  $\text{Co}(\text{CH}_3)_2^+$  and  $\text{Ni}(\text{CH}_3)_2^+$ . In order to obtain a reasonable fit between the theoretical and the experimental KERD for CO loss, a maximum contribution of 15%  $\text{Fe}(\text{CH}_3)_2^+$  and a minimum of 85%  $\text{Fe}^+\cdot\text{C}_2\text{H}_6$  to the reaction products was indicated.

Schultz and Armentrout<sup>36</sup> have done threshold collisional activation experiments on  $\text{FeC}_2\text{H}_6^+$  formed by two different reactions:  $\text{Fe}^+ + \text{ethane}$  (forming the  $\text{Fe}^+\cdot\text{C}_2\text{H}_6$  adduct) and  $\text{Fe}^+ + \text{acetone}$  (forming either the  $\text{Fe}^+\cdot\text{C}_2\text{H}_6$  adduct or  $\text{Fe}(\text{CH}_3)_2^+$ ). They believe that the  $\text{FeC}_2\text{H}_6^+$  product formed by decarbonylation of acetone is primarily the dimethyl structure with a maximum of 30%  $\text{Fe}^+\cdot\text{C}_2\text{H}_6$  being formed. Consequently, the maximum fraction of  $\text{M}(\text{CH}_3)_2^+$  isomer present in our work (15%) is significantly lower than the 70%  $\text{Fe}(\text{CH}_3)_2^+$  estimated to be formed in the ion beam studies.<sup>36</sup> This discrepancy may be due to an incorrect assumption made in interpreting the threshold collisional activation studies. In the ion beam studies, the fraction of  $\text{Fe}(\text{CH}_3)_2^+$  is determined from the observed differences in the cross section thresholds for  $\text{C}_2\text{H}_6$  and  $\text{CH}_3$  loss from the  $\text{FeC}_2\text{H}_6^+$  product formed by the two different methods and on differences observed in the cross sections for ligand exchange reactions with methane for  $\text{FeC}_2\text{H}_6^+$  formed by each process. Unfortunately, the thresholds for collision-induced dissociation of  $\text{FeC}_2\text{H}_6^+$  formed by decarbonylation of acetone were modeled assuming 100%  $\text{Fe}(\text{CH}_3)_2^+$ .

If the decarbonylation of acetone does indeed form only the dimethyl structure, it must isomerize (by C–C bond coupling) to the ethane adduct before losing  $\text{C}_2\text{H}_6$ . Schultz and Armentrout used the threshold for  $\text{C}_2\text{H}_6$  loss from  $\text{FeC}_2\text{H}_6^+$  formed from acetone (along with  $\text{H}_3\text{C}-\text{CH}_3$  and  $\text{Fe}^+-\text{CH}_3$  bond

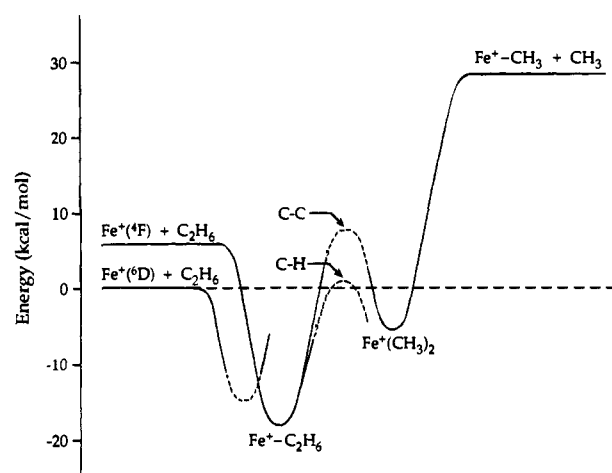


**Figure 5.** Relative energetics for C–H and C–C bond activation for  $\text{Fe}^+$  reacting with  $\text{C}_2\text{H}_6$ . The dashed portions of the curves indicate the C–H and C–C transition state energies are not precisely known, although the relative values are approximately correct (see text).

energies) to calculate a bond energy for  $\text{FeCH}_3^+-\text{CH}_3$ . Because it yields a value similar to that obtained by direct measurement of the threshold for  $\text{CH}_3$  loss from  $\text{FeC}_2\text{H}_6^+$  formed from acetone, they claim that the isomerization barrier between  $\text{Fe}(\text{CH}_3)_2^+$  and  $\text{Fe}^+\cdot\text{C}_2\text{H}_6$  must be below the asymptotic energy of  $\text{Fe}^+ + \text{C}_2\text{H}_6$ . However, this placement is not consistent with the following studies. First, it has been shown that  $\text{Fe}^+$  does not insert into the C–H bond of ethane (i.e., the C–H bond activation barrier is above the threshold energy of  $\text{Fe}^+ + \text{C}_2\text{H}_6$ ).<sup>9,55</sup> Second, threshold collisional activation of  $\text{Fe}^+\cdot\text{C}_3\text{H}_8$ ,<sup>24</sup> further experiments on propane,<sup>15</sup> and *ab initio* calculations<sup>25,26</sup> all indicate that C–C bond activation takes more energy than C–H bond activation. Thus, if the C–H bond activation barrier is above the energy of the reactants for  $\text{Fe}^+ + \text{C}_2\text{H}_6$ , then the C–C bond activation barrier is substantially above this energy. Figure 5 shows a revised surface including the large C–C bond activation barrier. The preponderance of data suggests a potential energy surface such as the one shown in Figure 5. Consequently, the threshold for  $\text{C}_2\text{H}_6$  loss measured by Schultz and Armentrout is due to direct  $\text{C}_2\text{H}_6$  loss from the ethane adduct and not from isomerization and subsequent dissociation of  $\text{Fe}(\text{CH}_3)_2^+$ .<sup>56</sup>

## Conclusions

Insight into the energetic requirements for  $\text{Fe}^+$ ,  $\text{Co}^+$ , and  $\text{Ni}^+$  reacting with acetone has been obtained by measuring product KERDs and comparing these results to the predictions of statistical phase space theory.

The low reaction efficiencies observed by Halle *et al.* for  $\text{Fe}^+$ ,  $\text{Co}^+$ , and  $\text{Ni}^+$  reacting with acetone<sup>27</sup> and statistical modeling of the experimental KERDs for the CO- and  $\text{C}_2\text{H}_6$ -loss channels indicate a rate-limiting, tight transition state exists somewhere along the reaction coordinate. We argue that this transition state is most likely initial C–C bond activation by the metal ion.

For the CO and  $\text{C}_2\text{H}_6$  loss channels, the rate-limiting transition state restricts the total angular momentum available to the

(53) *Ab initio* calculations of  $D_0(\text{M}^+-\text{CH}_3)_2$  show that these reactions are endothermic by about 6 kcal/mol (see ref 51). Taking into consideration the fact that the *ab initio* values for  $D_0(\text{M}^+-\text{CH}_3)_2$  could be approximately 10% too low, reactions between  $\text{M}^+$  and acetone to form  $\text{M}(\text{CH}_3)_2^+$  would be only slightly exothermic.

(54) The  $\text{C}_2\text{H}_6$ -loss channel for  $\text{Co}^+ + \text{acetone}$  has previously been modeled using phase space theory to determine a  $\text{Co}^+-\text{CO}$  bond energy of 31 kcal/mol (see ref 21). This value is unreasonably low due to the exclusion of the tight transition state in the theoretical model. In addition, the polarizability of acetone used to model the KERD in ref 21 was too low (see Appendix). Increasing the polarizability to take into account the effect of the dipole moment results in an even lower value,  $D_0(\text{Co}^+-\text{CO}) = 22$  kcal/mol, if a tight TS is not included. This argument lends further support that the tight transition state must be included in our theoretical model.

(55) A  $\text{C}_2\text{H}_4$  impurity was later found to be the cause of the exothermic portion of the cross section vs kinetic energy curve measured in the study discussed in ref 9 (Armentrout, P. B. Personal communication).

(56) It would be of interest to attempt to reanalyze the threshold ion beam data of Shultz and Armentrout using the limits set in this manuscript on the  $\text{FeC}_2\text{H}_6^+$  isomer distribution resulting from the reaction of  $\text{Fe}^+$  and acetone. Unfortunately we are not equipped to do so. There is no reason to believe a different isomer distribution is obtained in the ion source used in the ion beam work and the ion source used in our work.



**Table 5.** Input Parameters Used in Calculations

	(CH <sub>3</sub> ) <sub>2</sub> CO	(CD <sub>3</sub> ) <sub>2</sub> CO	CO	C <sub>2</sub> H <sub>6</sub>	C <sub>2</sub> D <sub>6</sub>	M <sup>+</sup> -C <sub>2</sub> H <sub>6</sub>	Co <sup>+</sup> -C <sub>2</sub> D <sub>6</sub>	M <sup>+</sup> -CO	M <sup>+</sup> -COC <sub>2</sub> H <sub>6</sub> <sup>a</sup>	Co <sup>+</sup> -COC <sub>2</sub> D <sub>6</sub> <sup>a</sup>
$\Delta H_0^\circ$ <sup>b</sup>	-48.1	-48.1	-27.2	-16.4	-16.4	245.3 <sup>c,d</sup> 233.3 <sup>d</sup>	285.1	220.6 <sup>d,e</sup> 216.2 <sup>d</sup> 213.2 <sup>d</sup>		
$B^f$	0.251	0.201	1.931	1.058	0.650	0.244 <sup>c</sup> 0.243	0.193	0.130 <sup>e</sup> 0.127 0.126	0.111 <sup>c,g</sup> 0.110 <sup>g</sup>	0.094 <sup>g</sup>
$\sigma^h$	2	2	1	6	6	1	1	1	1	1
$\alpha^i$	6.35	6.35	1.95	4.47	4.47					
$\nu^j$	3019 (2)	2264 (2)	2120	2954	2083	2954	2083	2170	3019 (2)	2264 (2)
	1731	2123 (2)		1388	1155	1388	1155	260	1435	2123 (2)
	1435	1732		995	843	995	843	200	1364 (2)	1080
	1364 (2)	1080		289	208	289	208	150	1066	1035 (2)
	1066	1035 (2)		2896	2087	2896	2087		777	887
	777	887		1379	1077	1379	1077		385	689
	385	689		2969 (2)	2226 (2)	2969 (2)	2226 (2)		2963	321
	2963	321		1468 (2)	1041 (2)	1468 (2)	1041 (2)		1426	2219
	1426	2219		1190 (2)	970 (2)	1190 (2)	970 (2)		877	1021
	877	1021		2985 (2)	2235 (2)	2985 (2)	2235 (2)		1410	669
	1410	669		1469 (2)	1081 (2)	1469 (2)	1081 (2)		1216	75
	1216	75		822 (2)	594 (2)	822 (2)	594 (2)		891	1242
	891	1242				260	260		530	1004
	530	1004				200	200		2972	724
	2972	724				150	150		1454	475
	1454	475							1091	2227
	1091	2227							484	1050
	484	1650							2973	960
	2937 (2)	960							105	405
	105	405							109	79
	109	79							100	100
									200	200
									150	150

<sup>a</sup> C-C bond activation transition state complex. <sup>b</sup> Heats of formation at 0 K in kcal/mol. The heats of formation for Fe<sup>+</sup>, Co<sup>+</sup>, and Ni<sup>+</sup> are 280, 282.5, and 278.4 kcal/mol, respectively. <sup>c</sup> First value for M = Fe, second for M = Ni. <sup>d</sup> From phase space calculations. <sup>e</sup> First value for M = Fe, second for M = Co, third for M = Ni. <sup>f</sup> Rotational constants in cm<sup>-1</sup>. <sup>g</sup> Rotational constant assuming M<sup>+</sup> inserts into the C-C bond perpendicularly to the plane of acetone. <sup>h</sup> Symmetry number. <sup>i</sup> Polarizability of neutral in Å<sup>3</sup>. <sup>j</sup> Vibrational frequencies in cm<sup>-1</sup>.

products, reducing the high-energy portion of the product KERD. Because the KERD is very sensitive to the energy of this transition state, its energy is accurately obtained by modeling the experimental distribution using statistical phase space theory. We have determined that it is located  $9 \pm 3$  kcal/mol below the Fe<sup>+</sup>, Co<sup>+</sup>, and Ni<sup>+</sup>/acetone asymptotic energies.

We find M<sup>+</sup>-CO binding energies of  $31.8 \pm 3$ ,  $39.1 \pm 3$ , and  $38.5 \pm 3$  kcal/mol for M = Fe, Co, and Ni, respectively, in good agreement with ion beam studies.<sup>38,40,41</sup> Our values of  $17.9 \pm 3$  and  $28.7 \pm 3$  kcal/mol for  $D_8^+(M^+-C_2H_6)$  with M = Fe and Ni, respectively, are also in good agreement with ion beam studies (for Fe<sup>+</sup>)<sup>36</sup> and with trends predicted by theory.<sup>23</sup> The rather large decrease in binding energy for C<sub>2</sub>H<sub>6</sub> ligands relative to CO occurs because there is back-donation from the metal to CO but not to C<sub>2</sub>H<sub>6</sub>.

Finally, we made what we feel are strong arguments that the rate-limiting transition state in M<sup>+</sup>/acetone is initial C-C bond activation. By comparing the details of the entrance channel energetics of the M<sup>+</sup>/acetone reactions with previously studied M<sup>+</sup>/alkane reactions we were able to conclude that initial C-C bond activation transition states are  $6 \pm 5$  kcal/mol higher in energy than initial C-H bond activation transition states. We are currently pursuing high-level *ab initio* calculations to firm up this point and other details of the potential energy surface described in this paper.

**Acknowledgment.** We gratefully acknowledge the support of the National Science Foundation under Grant No. CHE-9421176 and partial support of the Air Force Office of Scientific Research under Grant No. F49620-93-1-0305. We also thank Professor Peter Armentrout for communicating results prior to publication, Jason Perry for helpful discussions, and the reviewers for many useful suggestions.

## Appendix

Statistical phase space theory used to model the experimental KERDs has been previously outlined.<sup>21,30,31</sup> Figure 1 shows the schematic PES on which the calculations are based. Three transition states are included; two are loose orbiting transition states, one for the reactants and one for the products. The third is the rate-limiting, tight transition state. This transition state provides competition for the M<sup>+</sup>·acetone adduct to either go on to products or dissociate back to reactants. The probability of the M<sup>+</sup>·acetone complex with energy  $E$  and angular momentum  $J$  going on to products is given by eq A1:

$$P(E,J) = \frac{F^+(E,J)}{F_R^{\text{orb}}(E,J) + F^+(E,J)} \quad (\text{A1})$$

where  $F_R^{\text{orb}}(E,J)$  and  $F^+(E,J)$  are the microcanonical fluxes through the orbiting transition state back to reactants and through the tight transition state to go on to products, respectively.

Averaging over the energy and angular momentum distribution of the collision complex, the probability for forming products with translational energy  $E_t$  is given by A2:

$$P(E_t) = \frac{\int_0^\infty dE e^{-E/kT} \int_0^{J_{\text{max}}} dJ 2J F_R^{\text{orb}}(E,J) P(E,J) P(E,J;E_t)}{\int_0^\infty dE e^{-E/kT} \int_0^{J_{\text{max}}} dJ 2J F_R^{\text{orb}}(E,J)} \quad (\text{A2})$$

where  $P(E,J;E_t)$  is the fraction of molecules at energy  $E$  and angular momentum  $J$  decaying through the orbiting transition state to yield products with translational energy  $E_t$ .

The parameters needed for the calculations are given in Table 5. Rotational constants, polarizabilities and vibrational frequen-

cies were taken from the literature where possible or estimated from literature values of similar species.<sup>23,33,57</sup> The phase space calculations assume a point charge-point polarizable interaction between the reactants. Because acetone (which has a polarizability of  $6.35 \text{ \AA}^3$ ), has a large dipole moment, the polarizability used in the calculation can be increased to account for the effect of the dipole on the  $M^+$ /acetone interaction. The polarizability is increased (to  $25.1 \text{ \AA}^3$  in the case of acetone) such that the Langevin collision rate constant matches that determined by ADO theory.<sup>58,59</sup> However, when the tight transition state is included in the phase space calculations, the resulting KERDs are essentially independent of the polarizability over the range

(57) Shimanouchi, T. *Table of Molecular Vibrational Frequencies*; National Bureau of Standards: Washington, DC, 1972; Consolidated, Vol. I.

(58) Su, T.; Bowers, M. T. In *Gas Phase Ion Chemistry*; Bowers, M. T., Ed.; Academic Press: New York, 1979; Vol. 1, pp 84-118.

(59) Illies, A. J.; Jarrold, M. F.; Bass, L. M.; Bowers, M. T. *J. Am. Chem. Soc.* **1983**, *105*, 5775.

(60) Haynes, C. L.; Armentrout, P. B.; Perry, J. K.; Goddard, W. A., III *J. Phys. Chem.* **1995**, *99*, 6340.

of 6.35 to  $25.1 \text{ \AA}^3$ . This occurs because the C-C bond activation barrier blocks the high angular momentum collision complexes from going on to products. Thus, the polarizability of acetone was increased only in the unrestricted phase space calculations. Vibrational frequencies may be varied over a relatively large range of physically reasonable values without changing the KERD significantly. The main parameters influencing the KERD are  $\Delta H_{rxn}$  and  $\Delta E^\ddagger$ . For the systems studied here, the heats of formation of products and reactants were well known, including the  $Fe^+-C_2H_6$ <sup>36</sup> and  $Co^+-C_2H_6$ <sup>22,23,37</sup> and the  $Fe^+-CO$ <sup>33,38,39</sup>,  $Co^+-CO$ <sup>33,40</sup>, and  $Ni^+-CO$ <sup>33,41</sup> organometallic product ions. The binding energy for  $Co^+-C_2D_6$  is assumed to be the same as  $Co^+-C_2H_6$ . Finally, calculations were performed that explicitly included the time window for unimolecular reaction (i.e. the flight time from the magnet to the ESA). For reasonable choices of the vibrational frequencies of the adducts, only minor changes in  $\Delta E^\ddagger$  were observed ( $\leq 1 \text{ kcal/mol}$ ).

JA9510020